Published in final edited form as:
J Comp Neurol. 2008 September 1; 510(1): 100–116.

Contralateral Corticothalamic Projections from MI Whisker Cortex: Potential Route for Modulating Hemispheric Interactions

Kevin D. Alloway*, **Michelle L. Olson**, and **Jared B. Smith**
Department of Neural & Behavioral Sciences, Pennsylvania State University College of Medicine, Hershey, Pennsylvania 17033-2255

Abstract

Rat whisking behavior is characterized by high amounts of bilateral coordination in which whisker movements on both sides of the face are linked. To elucidate the neural substrate that might mediate this bilateral coordination, neuronal tracers were used to characterize the bilateral distribution of corticothalamic projections from primary motor (MI) cortex. Some rats received tracers in the MI whisker region, whereas others received tracers in the MI forepaw region. The MI whisker region projects bilaterally to the anteromedial (AM), ventromedial (VM), and ventrolateral (VL) nuclei, and to parts of the intralaminar nuclei. By contrast, the MI forepaw region sends virtually no projections to the contralateral thalamus. Consistent with these findings, bilateral injections of different tracers into the MI whisker region of each hemisphere produced tracer overlap on both sides of the thalamus. Furthermore, MI whisker projections to the contralateral thalamus terminate in close proximity to the thalamocortical neurons that project to the MI whisker region of that contralateral hemisphere. The terminal endings of the contralateral corticothalamic projections contain small synaptic varicosities and other features that resemble the modulator pathways described for other corticothalamic projection systems. In addition, tracer injections into AM, VM, and VL revealed dense clusters of labeled neurons in layer VI of the medial agranular (Agm) zone, which corresponds to the MI whisker region. These results suggest that projections from the MI whisker region to the contralateral thalamus may modulate the callosal interactions that are presumed to play a role in coordinating bilateral whisking behavior.

Indexing terms

bilateral coordination; drivers; interhemispheric; interthalamic; modulators; motor cortex; neuronal tracing; whisking

The classic view of interconnections between the thalamus and cortex has emphasized the ipsilateral projections that form reciprocal loops (Jones, 1985). Some of the earliest tracing studies, however, reported the presence of corticothalamic projections to the contralateral hemisphere, but the organization of these interhemispheric connections was rarely examined in any detail (De Vito, 1969; Leonard, 1969; Kunzle, 1976; Sotnichenko, 1976; Beckstead, 1979; Goldman, 1979; Kaitz and Robertson, 1981; Berman and Payne, 1982; Reep and Winans, 1982; Payne and Berman, 1984; Sakai and Tanaka, 1984).

More recent work in the rat has shown that primary motor (MI) cortex projects bilaterally to certain sites in the thalamus (Molinari et al., 1985; Rouiller et al., 1991; Shibata and Naito,

*Correspondence to: Dr. Kevin D. Alloway, Neural & Behavioral Sciences, H109, Hershey Medical Center, 500 University Dr., Hershey, PA 17033-2255, Email: kda1@psu.edu.
Associate Editor: Dr. Joseph L. Price

2005). These studies showed that projections from rat MI cortex terminate in several parts of the contralateral thalamus including the ventromedial (VM), ventrolateral (VL), and intralaminar nuclei. One report, however, indicates that the MI face region projects bilaterally to the thalamus, but the MI limb region projects only to the ipsilateral side (Rouiller et al., 1991). This anatomical distinction might be related to functional differences in bilateral coordination. Whereas exploratory whisking behavior is often characterized by synchronous bilateral movements of the whiskers at the same frequency (Gao et al., 2001; Sachdev et al., 2003; Sellien et al., 2005, Mitchinson et al., 2007), the limbs are much more likely to move independently.

Bilateral corticothalamic projections from the MI face region raise several issues concerning the structural and functional organization of the interconnections between the cortex and thalamus. The distribution of MI projections to the contralateral thalamus has not been examined with respect to the location of thalamocortical relay neurons that project to the contralateral MI cortex. Even if callosal connections are the primary mechanism for mediating communication between the MI regions in each hemisphere, an interhemispheric cortico-thalamo-cortical circuit could represent an additional route for reciprocal communication between the MI regions in each hemisphere.

If the thalamus provides a route for interhemispheric communication, the laminar origin of the MI projections to the contralateral thalamus, as well as their terminal morphology, could have a bearing on their functional significance. Growing evidence indicates that corticothalamic projections are subdivided into driver and modulator pathways that differ according to their laminar origin, terminal morphology, and physiological actions (Guillery, 1995; Sherman and Guillery, 1998; 2001; Guillery and Sherman, 2002). Whereas the corticothalamic drivers have thick axons with large terminals that originate in layer Vb, corticothalamic modulators have thin axons and small terminals that originate from layer VI.

To address these issues, we used neuronal tracing methods to analyze corticothalamic projections from rat MI cortex. In some rats we injected a single tracer into MI cortex and then characterized the bilateral distribution of the thalamic labeling. In other rats we injected two tracers bilaterally, either into both MI whisker regions or into both MI forepaw regions, and then characterized the tracer overlap in the thalamus. We also injected tracers into the thalamus to determine the laminar location of the labeled neurons in the contralateral MI cortex. Our results corroborate previous work indicating that the MI whisker region projects bilaterally to several nuclei in the thalamus, whereas the MI forepaw region projects almost exclusively to the ipsilateral thalamus (Roullier et al., 1991). Furthermore, the contralateral projections from the MI whisker region terminate in close proximity to thalamocortical neurons that project to the MI whisker region in that hemisphere. Finally, both the terminal morphology of these corticothalamic projections and their laminar origin in MI indicate that these neuronal projections act as modulators.

MATERIALS AND METHODS

All procedures conformed to NIH guidelines for the care and use of laboratory animals, and the complete protocol was approved by the Penn State Institutional Animal Care and Use Committee.

Animal surgery

Adult, male Sprague-Dawley rats (Charles River Co.), ranging from 350 to 695 g, were anesthetized with an intramuscular (IM) injection of ketamine (20 mg/kg) and xylazine (6 mg/kg). Supplements of these drugs were administered as needed throughout the surgery to suppress nociceptive withdrawal reflexes. Each rat also received atropine methyl nitrate (0.05

mg/kg, IM), chloramphenicol sodium succinate (50 mg/kg, IM), and dexamethasone sodium phosphate (5 mg/kg, IM), and was placed in a stereotaxic instrument. Heart rate and end-tidal CO_2 were monitored continuously, and body temperature was maintained at 37°C. The skin over the cranium was resected and the wound margins were infiltrated with 2% lidocaine. A craniotomy was made to locate appropriate sites for injecting neuronal tracers in the cortex or thalamus. After the tracer injections were complete and the wound margin was sutured, each animal received additional injections of atropine and dexamethasone before returning it to the animal colony where it was housed for 7–12 days.

MI tracer injections

A craniotomy was made at stereotaxic coordinates consistent with the whisker and forelimb regions in MI cortex, which range from 1.0–3.0 mm rostral and 0.5–3.0 mm lateral to bregma (Hall and Lindholm, 1974; Neafsey et al., 1986; Hoffer and Alloway, 2001; Brecht et al., 2004). Intracortical microstimulation (ICMS) was used to locate specific functional representations in MI cortex. Cathodal pulse trains of 80 ms (0.7-ms pulses and 3.3-ms interpulse intervals) were delivered through glass micropipettes that contained 3 M sodium chloride solution and had impedances of 0.3 to 1.8 Mh. After advancing the micropipette 1.7 mm below the pia, pulses of 100–150 μA were initially delivered to evoke twitches of the contralateral whiskers or forepaw. When clear muscle twitches were observed, the current was reduced to threshold levels (usually below 50 μA) until twitching disappeared. Multiple sites in MI cortex were tested with threshold current levels in each rat, and each response and its stereotaxic coordinates were recorded. Upon locating an appropriate site for a tracer injection, the stimulation electrode was removed and a tracer-filled pipette was inserted in its place.

Fluoro-ruby (FR) and Alexa-fluoro (AF) (Molecular Probes, D-1817 and D-2290, Eugene, Oregon) were injected bilaterally because these fluorescent tracers are transported in both the anterograde and retrograde directions. A 10% solution (in physiological saline) of FR or AF was pressure-injected from a glass pipette (40–120 μm tip) cemented to the needle of a Hamilton microsyringe. The injection plunger of the Hamilton microsyringe was controlled by a calibrated injector-holder (model 5000, Kopf Instruments, Tujunga, CA) that was attached to a micromanipulator on the stereotaxic frame. Injections were made at multiple depths located 1.2 to 1.7 mm below the pia, and the total volume of tracer injection ranged from 100 to 170 nl. These parameters produced small tracer deposits with a diameter of 399.0 ± 19.7 μm (mean ± SEM).

In other rats, biotinylated dextran amine (BDA) (Molecule Probes, D-7135, Eugene, Oregon) was iontophoretically injected into MI cortex of one hemisphere. In these cases, a 15% solution of BDA in 0.01 M phosphate buffered saline was placed in a glass pipette having an outer diameter of 40–80 μm, and positive current (4–6 μA) pulses were applied in alternating on-off intervals of 7 seconds for 6 to 8 minutes at each cortical depth. In most penetrations BDA was injected at 3 or 4 depths located 1.2 to 1.7 mm below the cortical surface. In rats receiving BDA, the injections were often made at 2 or 3 penetrations located within 200 μm of the most effective ICMS site.

SI tracer injections

In two rats, BDA was deposited into multiple sites of SI barrel cortex. After using multiunit recording techniques to identify SI sites that responded to manual deflections of the whiskers, BDA was injected into the SI barrel field using methods similar to those described for MI (see above). A pipette filled with 15% BDA solution was used to make tracer injections at 3 cortical depths (1.2, 0.8, and 0.4 mm below the pial surface). At each depth, BDA was injected for 6–8 minutes. This was done at 4 sites in barrel cortex to produce a large tracer deposit that extended 1–2 mm in diameter and labeled the majority of the barrel field.

Thalamus tracer injections

In another two rats, fluoro-gold (FG) was iontophoretically injected into the thalamus to reveal the topography and laminar location of labeled neurons in the contralateral MI cortex. After making a craniotomy located 2.0 mm caudal and 1.2 mm lateral to bregma, which corresponds to the stereotaxic position of the AM, VL, and VM nuclei (Paxinos and Watson, 1986), a pipette filled with 2% FG was lowered 6.8 mm below the pia. While the pipette was advanced into the thalamus, a retention current (− 5 μA) was applied to the FG solution to prevent unwanted leakage. After reaching the desired depth, an injection of FG was made by applying 4 μA for 5 minutes, 3 μA for 5 minutes, and then 2 μA for 30 minutes. The pipette was then raised 1.0 mm and a second deposit was made by applying a current of 2 μA for 15 minutes. The retention current was reapplied when the pipette was withdrawn from the brain. These parameters produced FG deposits that were 1 mm wide and 2.0 mm in height.

Histology

Each rat was anesthetized with sodium pentobarbital (100 mg/kg, i.p.) and transcardially perfused with physiological saline (500 ml) followed by 4% paraformaldehyde in 0.1 M phosphate buffer (400 ml) and 4% paraformaldehyde with 10% sucrose (350–400 ml). The brain was removed and refrigerated for 36 hours in 4% paraformaldehyde with 30% sucrose. To distinguish the right and left sides during section mounting, a small slit was made in the ventral cortex and brainstem of the left hemisphere. The entire brain was cut coronally in serially-ordered sections that were 60–80 μm thick. Sections were serially processed at regular intervals; one or two series of sections were processed for tracer labeling and another series was either stained with thionin or processed for cytochrome oxidase to reveal the thalamic nuclei (Wong-Riley, 1979; Land and Simons, 1985), which were identified according to Paxinos and Watson (1986).

Sections processed for BDA were handled as described previously (Alloway et al., 1998; Kincaid and Wilson, 1996). After gently agitating the sections in 0.3% H_2O_2 and then in 0.1 M PB with 0.3% Triton-X100 (pH 7.4), the sections were incubated in an activated avidin-biotinylated horseradish peroxidase solution (Vector Novocastra Laboratories, Burlingame, CA) for 2–4 hours. The sections were rinsed in 0.1 M PB and then incubated with 0.05% diaminobenzidine (DAB), 0.005% H_2O_2, and 0.04% $NiCl_2$ in 0.1M Tris buffer (pH 7.1) for 9–12 minutes. After another set of washes in).1M PB, the sections were mounted on gel-coated slides, dried overnight, and briefly dipped in alcohol and xylene prior to being coverslipped with Cytoseal. Neurons and terminals labeled by BDA were viewed using conventional light microscopy.

Sections processed for fluorescent labeling were mounted in serial order on gel-coated slides. After drying overnight, the sections were briefly dipped in alcohol and xylene, and were then coverslipped with Cytoseal. A combined fluorescein isothiocyanate/tetrarhodamine isothiocyanate (FITC/TRITC) filter set (51004v2, Chroma Technology; Rockingham, VT) was used to visualize fluorescent AF- and FR-labeled processes simultaneously.

Anatomical analysis

Sections with labeled neurons and terminals were digitally reconstructed using the AccuStage system (St. Paul, MN) in conjunction with an Olympus light microscope (BH-2) equipped with a variety of objectives. Labeled neurons and terminals were plotted with respect to nuclear boundaries and other anatomical landmarks such as the corpus callosum and lateral ventricle. The resulting digital reconstructions of the labeling and anatomic landmarks were stored on computer disk for subsequent analysis.

For quantitative analysis of the labeled neurons and terminals in the thalamus, the reconstructed plots were subdivided into an array of square bins as described earlier (Alloway et al., 2003; Hoffer et al., 2005; Chakrabarti and Alloway, 2006). Bins that contained labeled processes were counted for statistical analysis. In one analysis, we counted the total number of bins that contained terminals labeled by one tracer (BDA, AF, or FR) and then determined the proportion of the bins that were in the contralateral thalamus. For animals that received bilateral injections of fluorescent tracers, we calculated the amount of overlapping FR- and AF-labeled terminals in the thalamus. Thus, bins that contained AF- or FR-labeled terminals were colored green or red, respectively, whereas those that contained both tracers were colored white. The green, red, and white bin counts were summed, and the number of white bins (ie. labeled overlap) on both sides of the thalamus was expressed as a proportion of the total sum of white, red, and green bins.

We used a similar method to analyze the proximity of projections to the labeled soma in the contralateral thalamus. For example, bins that contained only AF-labeled soma or FR-labeled terminals were colored green or red, respectively, whereas bins that contained both AF-labeled soma and FR-labeled terminals were colored white. For each hemisphere, the number of white bins (which contain terminals labeled by one tracer and soma labeled by the other tracer) was expressed as a proportion of the total number of white, red, and green bins.

Photomicrographs of labeled material were obtained with three microscopic systems. For low power photomicrographs of Nissl material or BDA labeling, we used a Cool Snap HQ CCD digital camera (Roper Scientific, Tucson, AZ) mounted on a BH-2 Olympus microscope that was equipped with 1X, 2X, and 4X objectives. For higher power photomicrographs of BDA labeling, we used a SPOT RT Camera system (Diagnostic Instruments, Inc., Sterling Heights, MI) mounted on a BX50 Olympus Microscope equipped with 60X and 100X oil immersion objectives. To obtain high power images of neuronal processes labeled by FR or AF, we used a Leica confocal microscope (TCS SP2 AOBS, Leica Microsystems, Manheim, Germany) that was equipped with a 543 nm laser for FR excitation (detection band set at 565 to 630 nm) and a 488 nm laser for AF excitation (detection band set at 499 to 565 nm). Optical sections of these fluorescent images were reconstructed by the Leica software and were saved at a resolution of 512 × 512 pixels. All images from conventional and confocal microscopy were saved as TIF files, which were imported into a software program (Deneba Systems, Inc., Canvas X; Miami, FL) in which brightness and contrast were adjusted to portray the images as they appeared through the microscope.

RESULTS

As indicated by Table 1, corticothalamic projections from MI cortex were analyzed in 24 rats. Among these cases, 12 rats were injected with a single tracer in the right MI cortex and 12 rats received bilateral injections of a different tracer in MI of each hemisphere. Additional rats received tracer injections in MI cortex but were not included in our analysis (n = 12) because the injections were either unsuccessful or the subsequent histology was problematic. To compare the terminal morphology of corticothalamic projections from MI and SI, 2 rats received tracer injections in the SI whisker barrel field. We also injected FG into one side of the thalamus of 2 rats to determine the laminar location and topography of labeled neurons in the contralateral MI cortex.

Among the rats that received tracers in MI cortex, the tracers were deposited into the forepaw or whisker representations. To locate the border between the whisker and forepaw regions, ICMS was tested at multiple sites. Although ICMS occasionally evoked simultaneous twitches of both the whiskers and forepaw, movements were usually restricted to only site on the body. To avoid tracer diffusion into both regions, injections were made only at sites that evoked

movements of the same body part. Based on this criterion, our analysis was conducted on 15 rats in which tracers were placed in the MI whisker region and on another 9 rats that received injections in the MI forepaw region (see Table 1).

MI whisker region in medial agranular cortex

Among the 12 rats that received unilateral tracer injections, 9 involved tracer deposits in the MI whisker representation. An example of an injection into the MI whisker region is shown in Fig. 1. In this case (BN27), a dense deposit of BDA was placed at a site in which ICMS evoked movements of contralateral whiskers D1, D2, and E2. The tracer occupied a wedge-shaped area that infiltrated virtually all cortical layers, but it did not diffuse into the underlying white matter. Consistent with the view that BDA is preferentially transported in the anterograde direction, we observed virtually no BDA-labeled soma in the surrounding cortex or in the opposite cortical hemisphere. Comparison of both hemispheres indicated that the wedge-shaped BDA deposit was matched by a similar pattern of BDA-labeled terminals in the opposite hemisphere (see Fig. 1A). Inspection of multiple sections close to the injection site revealed a bundle of labeled fibers that crossed the midline through the corpus callosum and then terminated in the corresponding MI region in the left hemisphere. Similar patterns were observed in other cases that received unilateral injections.

As shown by panels B, C, and D in Fig. 1, we examined the tracer deposits with respect to the surrounding cytoarchitecture. When tracers were placed in MI sites that evoked whisker movements, the tracer deposit was located in the medial agranular (Agm) zone, which is marked by a high density of neurons in a relatively thick layer V. By comparison, when we injected tracers into MI regions that evoked movements of the forepaw, the injected area was located in the lateral agranular (Agl) zone, which is characterized by a thin layer V and a relatively thick layer III. These findings corroborate a recent study that compared MI cytoarchitecture with detailed maps of the motor responses produced by ICMS (Brecht et al., 2004). The cytoarchitectonic features that define the border between Agm and Agl change gradually, however, and tracer deposits at some sites that evoked whisker movements were observed in the transitional region between Agm and Agl. Nonetheless, in all cases involving injections in the forepaw region, virtually the entire tracer deposit appeared lateral to this transitional region.

Bilateral corticothalamic projections from the MI whisker region

Tracer injections in the MI whisker region produced a distinct bilateral pattern of labeled axons and their terminals in the thalamus. Figure 2 shows the bilateral corticothalamic labeling pattern produced by the tracer injection illustrated in Fig. 1. Consistent with previous descriptions of MI projections to the ipsilateral thalamus (Aldes, 1988; Miyashita et al., 1995), Fig. 2 depicts the dense labeling that appeared in the ipsilateral ventrolateral (VL) and ventromedial (VM) nuclei, both of which are considered motor-specific regions (Groenewegen and Witter, 2004). Ipsilateral labeling was also dense in the centrolateral (CL) and paracentral (PC) intralaminar nuclei, and in the anteromedial (AM) and interanteromedial (IAM) nuclei, the latter of which represents the fusion of the medial halves of the AM nuclei at the midsagittal plane (Groenewegen and Witter, 2004). Although not depicted in Fig. 2, dense ipsilateral labeling was seen more caudally in the medial part of the posterior complex (POm) and in the rostral part of the reticular (Ret) nucleus. Labeling was more moderate in the ipsilateral zona incerta (ZI), and was noticeably less dense in the ventral and lateral parts of the mediodorsal (MD) nucleus and in the nucleus reuniens (Re). Consistent with the selectivity of BDA for labeling axons only in the anterograde direction, very few neurons in the ipsilateral thalamus were labeled by BDA (Fig 2F).

Labeled terminals were observed in some of the same nuclei in the contralateral thalamus, but the labeling was generally less dense than in the ipsilateral thalamus. The MI projections to

the contralateral thalamus appeared approximately 2.0 to 4.0 mm caudal to bregma, where bundles of labeled fibers traversed the midline through the IAM nucleus and terminated in the adjacent AM nucleus and in other nuclei located more laterally. As shown in Fig. 2, the density of AM labeling was similar on both sides of the thalamus. Labeled fibers coursed beyond the AM nucleus, but the density of this contralateral labeling was noticeably lower than in the AM nucleus. Many of these labeled fibers proceeded ventrally and then terminated in the contralateral VM nucleus (see Fig. 2C and E). A less dense collection of labeled fibers proceeded dorsolaterally from the AM nucleus and then terminated in the PC and CL regions of the intralaminar nuclei. Although contralateral labeling declined markedly where the lateral edges of the AM and VM nuclei joined the medial border of the VL nucleus, several labeled fibers crossed this border and terminated in the medial and dorsal parts of the VL nucleus (see Fig. 2C and D).

The contralateral thalamic labeling depicted in Fig. 2 is unlikely to originate from retrogradely-labeled thalamic neurons that are ipsilateral to the MI injection site. Although thalamocortical relay neurons might send collateral axonal projections to both the MI injection site and the contralateral thalamus, very few BDA-labeled neurons appeared in the AM, VM, and VL nuclei of the ipsilateral thalamus (Fig. 2F). Furthermore, despite very dense terminal labeling in PC and CL, no retrogradely-labeled neurons appeared in these intralaminar nuclei. Hence, the small number of BDA-labeled neurons in the ipsilateral thalamus could not account for the dense plexus of labeled terminals seen in the contralateral thalamus.

Overlapping corticothalamic projections from the MI whisker region

To confirm that ipsilateral and contralateral corticothalamic projections terminate in some of the same nuclei, we bilaterally injected different anterograde tracers into the MI whisker region of each hemisphere. Figure 3 illustrates the location of fluorescent tracer injections in the left and right MI whisker regions of case BN11. Although the FR tracer injection was slightly larger than the AF injection, both tracers were placed in corresponding cortical regions in which ICMS evoked movements of the B1 or B2 whiskers (see case BN11 in Table 1).

The bilateral labeling patterns of each tracer indicate that corticothalamic projections from both MI whisker regions overlap in certain thalamic nuclei. As seen in Fig. 4A, FR-and AF-labeled projections occupied symmetrical regions in many parts of the rostral thalamus. Although FR-labeled projections were more numerous and terminated more extensively in the contralateral thalamus than the contralateral projections from the AF injection site, intermingled AF- and FR-labeled terminals were observed in both specific (VM, VL) and non-specific (AM, PC, CL) thalamic nuclei. When the digital reconstructions in Fig. 4A were subdivided into 50 μm^2 bins, the proportion of bins that contained both AF- and FR-labeled terminals varied from 18.2 to 25.5% (see Fig. 4B). When the labeling in all thalamic sections from case BN11 were analyzed, tracer overlap represented 15.1% of the total thalamic area that was occupied by the tracers.

Cortico-thalamo-cortical circuits

When AF and FR were injected bilaterally into MI cortex, many of the labeled projections to the contralateral thalamus terminated near thalamocortical neurons labeled by the other tracer. Figure 5, for example, illustrates the distribution of retrogradely-labeled soma and anterogradely-labeled terminals in case BN11. Consistent with previous reports characterizing the distribution of thalamocortical relay neurons that project to MI (Molinari et al., 1985), virtually all retrogradely-labeled neurons were ipsilateral to the MI injection site. Labeled neurons were densest in the VL nucleus, but were also present in VM, MD, AM, IAM, and in the intralaminar nuclei. Many labeled soma were located very close to the thalamic midline, but were rarely seen contralateral to the injection site.

Most regions that received corticothalamic projections from the contralateral MI injection site contained neuronal cell bodies labeled by the other tracer. Thus, as seen in the reconstruction illustrated in Fig. 5A, AF-labeled soma in VL, VM, MD, PC, CL, AM, and IAM on the left side are intermingled with FR-labeled corticothalamic projections from the right MI whisker region. Furthermore, high power photomicrographs of AF-labeled neurons in VL, VM, and IAM of case BN 11 confirm that they are surrounded by FR-labeled terminals (see panels C, D, and E in Fig. 5).

To assess the feasibility of interhemispheric cortico-thalamo-cortical circuits, we quantified the proximity of labeled corticothalamic projections with respect to thalamocortical neurons labeled by the other tracer. For this analysis, ipsilateral corticothalamic terminals were removed from the thalamic reconstructions as shown in Fig. 6A. Hence, for each side of the thalamic reconstruction, retrogradely-labeled neurons are shown only with respect to corticothalamic projections that originate from the contralateral MI. We then subdivided each half of the thalamic reconstruction into an array of square bins and calculated the proportion of bins that contained both tracers (see panels B and C in Fig. 6). As shown in Fig. 6, an array of 100 μm^2 bins revealed interhemispheric corticothalamic and thalamocortical overlap in more than 10% of the labeled bins.

Corticothalamic projections from MI forepaw regions

To determine whether all functional regions in MI cortex project bilaterally to the thalamus, we also placed tracers into MI sites in which ICMS evoked isolated movements of the contralateral forepaw. Figure 7 illustrates a case (BN16) in which AF and FR were separately injected into the MI forepaw regions of the left and right hemispheres, respectively. As the photomicrographs indicate, both tracer injections occupied corresponding cortical areas in the two hemispheres.

Reconstructions of the corticothalamic labeling patterns indicate that the MI forepaw region sends few projections to the contralateral thalamus. As shown in Fig. 8, corticothalamic projections from the MI forepaw region innervate extensive parts of the ipsilateral thalamus including motor-specific nuclei such as VL and VM. In addition, ipsilateral corticothalamic labeling appeared in POm, in parts of Ret, in AM, and in the intralaminar nuclei, PC and CL. Sparse ipsilateral labeling was also present in the very rostral part of the ventroposterolateral (VPL) nucleus. Very few labeled corticothalamic axons, however, crossed the midline and terminated in the contralateral thalamus. Consistent with this, quantitative analysis of corticothalamic overlap in case BN16 revealed few thalamic sites that received projections from both MI injection sites. When the thalamic reconstructions in Fig. 8A were subdivided into 50 μm^2 bins, one section displayed tracer overlap in 2.1% of the bins, but the other section displayed no overlap. When all thalamic sections for case BN16 were analyzed, the amount of tracer overlap represented only 0.47% of the thalamic area that contained labeled projections.

Quantitative analysis of MI whisker and forepaw projections

Several statistical analyses confirmed that the MI whisker region sends more projections to the contralateral thalamus than the MI forepaw region. When the tracer was placed in the MI whisker region (n = 21), the mean amount of contralateral thalamic labeling across all cases represented 11.6 ± 1.8% (mean ± SEM) of the total thalamic area that contained terminal labeling. By comparison, only 2.3 ± 0.7% of the thalamic area that contained labeled projections from the MI forepaw region (n = 15) was on the contralateral side (see Fig. 9A). This functional difference in the areal extent of contralateral labeling was significant ($t = 4.19$, $p < 0.0001$).

Consistent with differences in the proportion of projections to the contralateral thalamus, bilateral tracer injections in the MI whisker regions produced more tracer overlap than bilateral

injections in the MI forepaw regions. As shown in Fig. 9B, mean tracer overlap in the thalamus was 6.1 ± 2.1% when different tracers were injected into the MI whisker regions of each hemisphere (n = 6), but was only 0.5 ± 0.6% when both MI forepaw regions were injected (n = 6). Statistical analysis confirmed that this difference was significant ($t = 2.71$, $p < 0.05$).

Other comparisons of the thalamic labeling patterns produced by bilateral tracer injections underscore the functional differences in interhemispheric connectivity of the whisker and forepaw regions in MI. To determine if labeled projections to the contralateral thalamus might innervate thalamocortical relay neurons labeled by the other tracer, we analyzed the number of square bins in which retrogradely-labeled neurons were intermingled with corticothalamic projections from the contralateral MI injection site (see Fig. 6). Because dendrites of thalamocortical neurons in VM, VL, the intralaminar region and other thalamic nuclei may extend 200 μm or more from the cell body (Yamamoto et al., 1985;Ohara and Havton, 1994), we used several bin sizes to analyze the proximity of terminals labeled by one tracer with respect to thalamocortical neurons labeled by the other tracer. Regardless of bin size, the thalamic area occupied by terminals and soma labeled by different tracers was higher following tracer injections into the MI whisker region (Fig. 9C). An analysis of variance confirmed that the proximity of labeled terminals with respect to labeled soma in the contralateral thalamus was affected by the functional location (whisker vs. forepaw regions) of the bilateral injections in MI cortex ($F = 31.6$, $p < 0.0001$). An increase in bin size also had a significant effect on the amount of terminal-soma overlap ($F = 12.9$, $p < 0.0001$). Finally, we detected a significant interaction between the tracer injection sites and the size of the bins used to measure terminal-soma overlap ($F = 4.4$, $p < 0.01$).

Terminal morphology

Several reports indicate that corticothalamic projections to higher-order thalamic nuclei have morphologic characteristics that distinguish them from the corticothalamic projections that gate the relay of information through the sensory-specific thalamic nuclei (Guillery, 1995; Sherman and Guillery, 2001). Whereas corticothalamic projections from SI to the ventrobasal complex are characterized by thin axons with small terminals, those projecting from SI to the nucleus POm have thicker axons with larger terminal boutons (Bourassa et al., 1995; Reichova and Sherman, 2004). In fact, differences in the physiological effects of these projections have prompted the designation of the large terminals as “drivers” whereas the small terminals are “modulators.” Therefore, we compared the terminals of corticothalamic projections from sensorimotor cortex to the ipsilateral nucleus POm with the terminals of MI projections to the contralateral thalamus.

Consistent with previous reports (Hoogland et al., 1991; Bourassa et al., 1995), labeled projections from SI barrel cortex to the ipsilateral POm have enormous terminal endings in which the terminal boutons and other axonal varicosities are 4 or 5 μm in diameter (see Fig. 10A). Some small terminal boutons were observed in POm after tracer injections in SI, but the larger terminals were far more prevalent. Compared to these SI projections to POm, the MI projections to the ipsilateral POm had terminal boutons that were noticeably smaller. As shown in Fig. 10B, the largest of the MI projection terminals in POm usually ranged between 2 and 3 μm in diameter. These moderately large terminals were relatively rare, however, and were located in a small part of POm as described previously (Rouiller et al., 1991). Much smaller terminal boutons, which had diameters no larger than 1 μm, were much more numerous in POm. In addition to the small terminal boutons, equally small (1μm or less) beaded varicosities frequently appeared along the labeled axons in POm, either as axonal enlargements or as “drumstick-shaped” terminals that appeared at the end of short axonal branches that extended 4 or 5 μm from the main axon. Hence, the labeled projections from MI to the ipsilateral POm

had large and small terminals that appeared to represent a combination of drivers and modulators.

By contrast, the MI projections to the contralateral thalamus were characterized exclusively by thin axons with small terminal boutons and small drumstick-shaped varicosities that resembled modulator projections. As illustrated by Fig. 11, MI projections to the contralateral thalamus had terminal boutons and axonal varicosities that were generally 1 μm or less in diameter. In fact, the small size of these axons and their terminal endings made it difficult to acquire photomicrographs that accurately depicted their morphologic structure. Useful images were obtained only from sparsely-labeled sections or from regions at the fringe of the densest labeling where the labeling could be visualized within a single focal plane located against a relatively uniform background. Nonetheless, regardless of whether we examined regions of dense or sparse labeling, all of the labeled projections from MI to the contralateral thalamus, including projections to the AM, PC, PL, VL, and VM nuclei, were characterized by thin axons with small varicosities.

Topography and laminar location of labeled neurons in MI cortex

The tracer FG, which is transported only in the retrograde direction, was iontophoretically injected into the right thalamus of two rats so that we could characterize the topography and laminar location of retrogradely labeled neurons in MI cortex. As shown by one of these cases in Fig. 12, FG was injected into AM, VM, the medial part of VL, and the ventral part of AV. Although the intralaminar nuclei are not easily visualized, it is likely that FG also infiltrated parts of the PC and CL nuclei.

Many FG-labeled neurons were observed in the ipsilateral thalamus around the injection site, but labeled neurons in the contralateral thalamus were restricted to the reticular nucleus and the zona incerta. In addition to labeling many thalamic neurons close to the fringe of the tracer deposit, FG caused intense labeling of more distant neurons that lined the ipsilateral side of the thalamic midline (Fig. 12C). By contrast, extremely few FG-labeled neurons were seen in the contralateral thalamus at the same rostrocaudal level as the FG deposit. Only a couple of brightly-labeled neurons, as well as a few pale neurons, appeared in the zona incerta of the contralateral thalamus (see arrow in Fig. 12C). In the rostral part of the thalamus, however, a dense cluster of bright, FG-labeled neurons appeared in the reticular nucleus as described previously (Raos and Bentivoglio, 1993).

Examination of MI cortex in both hemispheres revealed differential patterns of labeled neurons in Agm of the ipsilateral and contralateral hemispheres. As illustrated by Fig. 13, retrogradely-labeled neurons in the ipsilateral MI cortex formed two distinct layers. As seen in Fig. 13 C, most of the FG-labeled neurons in the ipsilateral MI occupied a relatively thick region in layer VI. A second layer of FG-labeled neurons occupied a thin region that was separated from the dense labeling in layer VI. Because layer V in the MI whisker region is relatively thick, this second sheet of FG-labeled neurons appeared to be in layer Vb. By comparison, FG-labeled neurons in the contralateral MI cortex were observed only in layer VI (see Fig. 13A).

The labeled neurons in both hemispheres were observed in the medial part of the agranular zone (Fig 13D and 13F). Substantial labeling also appeared more ventrally in the cingulate cortex, possibly because some tracer diffused into parts of the anterior nuclear complex that receive corticothalamic projections from the cingulate cortex (Seki, Zyo, 1984; Shibata H, Naito J. 2005). The labeling in both hemispheres was also characterized by a sharp drop in the density of labeled neurons on the lateral side, presumably because of the precise pattern of functional connections between the thalamus and cortex. Nonetheless, the edges of the labeled region in MI extended somewhat further laterally on the ipsilateral side than on the contralateral side.

DISCUSSION

Our data confirm and extend previous reports showing that MI cortex projects bilaterally to certain thalamic nuclei. In contrast to the MI forepaw region, which projects almost exclusively to the ipsilateral thalamus, the MI whisker region projects bilaterally to the AM, VM, VL, and certain intralaminar nuclei. Following bilateral injections of different tracers into the MI whisker region of each hemisphere, these thalamic nuclei receive overlapping projections from both hemispheres. These dual tracing experiments indicate that MI projections to the contralateral thalamus terminate close to many thalamocortical neurons that project to the MI cortex in that hemisphere. Visualization of these contralateral terminals revealed small boutons and beaded varicosities that resemble the modulator inputs described for other corticothalamic pathways. Consistent with this view, retrograde tracer injections into the thalamus revealed labeled neurons in layer VI of the contralateral MI cortex. Collectively, these findings suggest that an interhemispheric cortico-thalamo-cortical circuit may modulate the callosal connections that mediate direct interactions between the MI whisker regions in each hemisphere.

Hypothetical functions of the contralateral corticothalamic projections

The differential patterns of corticothalamic projections from the MI whisker and forepaw regions suggest fundamental differences in the neural control of the whiskers and forelimbs. Distinctions in the neural substrate controlling the whiskers and forelimbs are probably related to behavioral differences in the bilateral coordination of these body parts. High speed videography has shown that exploratory whisking usually consists of bilateral movements in which whiskers on each side of the face move simultaneously, often at the same frequency and amplitude (Gao et al., 2001; Sachdev et al., 2003; Sellien et al., 2005; Mitchinson et al., 2007). Asymmetric whisker movements may occur in response to unilateral whisker stimulation, but whisker motion on one side of the head is still linked to predictable movements on the other side (Sachdev et al., 2003; Mitchinson et al., 2007). Moreover, even when bilateral whisker movements are out-of-phase with each other during lateral head movements, the whiskers often move at the same frequency (Towal and Hartmann, 2006). By contrast, although both forelimbs are often coordinated during grooming and other behaviors, limb movements across the two sides of the body are more likely to be dissociated from each other. Thus, rats and other rodents frequently engage in manual behaviors such as reaching, bar-pressing, and other unilateral paw movements.

The bilateral corticothalamic projections from the MI whisker region suggest that some whisking-related behaviors must depend on interhemispheric coordination. Although our study does not indicate the precise nature of this dependence, ethologic considerations may narrow the potential list of behaviors and the neural mechanisms that mediate them. Whisking behavior, for example, is strongly coordinated with sniffing and head movements (Welker, 1964; Kepecs et al., 2006). The sensory inputs from the whiskers, nose, and vestibular system provide essential feedback for regulating subsequent movements of these body parts. Because whisking, sniffing, and related head movements require bilateral activation of many midline muscles, the degree of coordination amongst these muscles should be quite high.

This line of reasoning suggests that some interhemispheric connections must play a role in mediating or modulating the bilateral coordination of whisking-related behaviors. Whereas callosal projections provide direct interconnections between the MI regions in each hemisphere, an interhemispheric cortico-thalamo-cortical circuit represents a second route that could modulate the coordination of MI activity across the two hemispheres. The exact functions of this multisynaptic circuit are unclear, however. Depending on the synaptic details, especially with respect to the inhibitory neurons in the thalamus and MI cortex, this cortico-thalamo-cortical loop could enhance synchronization of bilateral whisker movements or, alternatively,

could mediate the decoupling of bilateral whisker movements in response to head movements or unilateral whisker stimulation (Towal and Hartmann, 2006; Mitchinson et al., 2007).

Functions of the contralateral corticothalamic projection targets

Projections from the MI whisker region to the contralateral VL and VM nuclei are likely to have some role in modulating the transmission of motor information from the thalamus to MI cortex. Both VM and VL are considered motor-specific nuclei in the thalamus because of their afferent and efferent connections with several components of the motor system (Groenewegen and Witter, 2004). Because the contralateral projections from MI terminate much more densely in VM than in VL, we place greater emphasis on VM when considering the functional roles of this interhemispheric loop. The nucleus VM receives inputs from the entopeduncular nucleus (medial segment of the globus pallidus) and from the substantia nigra pars reticulata (Carter and Fibiger, 1978; Herkenham, 1979; Deniau et al., 1994). The nucleus VM also receives inputs from the deep layers of the superior colliculus and the deep mesencephalic nucleus (Herkenham, 1979; Krout et al., 2001), brainstem structures known to receive inputs from the MI whisker region (Hattox et al., 2002). In addition, the nucleus VM receives some inputs from the cerebellum (Angaut et al., 1985), which is consistent with the projections from MI cortex to the pontocerebellar system (Leergaard et al., 2004). Although some outputs from the nucleus VM terminate in the deep layers of MI cortex (Arbuthnott et al., 1990), VM projections throughout frontal cortex are known for terminating in layer I (Herkenham, 1979; Desbois and Villanueva, 2001, Mitchell and Cauller, 2001). These connections, as well as the fact that the nucleus VM receives inputs from several caudal nuclei in the reticular brain stem (Villanueva et al., 1998), have prompted the suggestion that VM is involved in attentional mechanisms that prepare the motor system for specific behavioral responses (Groenewegen and Witter, 2004).

The nucleus AM is part of the anterior nuclear complex, which is considered one of several association regions in the thalamus (Groenewegen and Witter, 2004; for an alternative view, see Sherman and Guillery, 2001). We found that MI projections to the contralateral AM nucleus are noticeably denser than the MI projections to any of the other contralateral thalamic targets. Furthermore, MI projections to the nucleus AM are almost equally dense on the ipsilateral and contralateral sides of the thalamus. The afferent and efferent connections of the anterior nuclear complex, including the AM nucleus, suggest that this complex represents an extended hippocampal system that processes information related to spatial orientation and spatial memory (Aggleton and Brown, 1999). Thus, the AM nucleus and other anterior nuclei receive inputs from the limbic cortex (in the medial wall of the cerebral hemisphere), from the parahippocampal region, and from the mammillary nuclei (Swanson and Cowan, 1977; Seki and Zyo, 1984; Witter et al., 1990; Shibata, 1992). Outputs from the AM nucleus project to the cingulate cortex, especially its rostral subdivisions, and to visual cortical area 18 (Shibata, 1993; Van Groen et al., 1999; Vogt et al., 2004). Consistent with its hippocampal circuit connections, which probably mediate attentional processes related to spatial memories, electrophysiological studies indicate that neurons in AM and other anterior nuclei encode the spatial orientation of the head within the horizontal plane (Mizumori and Williams, 1993; Aggleton et al., 1996; Blair et al., 1997). Given the relationship between horizontal head movements and subsequent shifts in bilateral whisker coordination (Towal and Hartmann, 2006), it is reasonable that the MI whisker region should have bilateral connections with brain regions that regulate head direction.

Substantial data indicate that the PC and CL nuclei, which represent intralaminar regions, are reciprocally connected with the contralateral MI whisker region. These intralaminar nuclei receive ascending inputs from multiple brainstem regions and, in turn, project to cortex and many subcortical structures including the basal ganglia, amygdala, and hypothalamus (Groenewegen and Witter, 2004). More specifically, the PC and CL nuclei project to the

prefrontal and anterior cingulate cortices, both of which play a critical role in arousal and cognitive awareness (Bentivoglio et al., 1991; Van der Werf et al., 2002). Part of these projections also terminate in regions that were originally identified as secondary motor cortex (Berendse and Groenewegen, 1991; Van der Werf et al., 2002), but clearly correspond to Agm, which has been identified here and elsewhere as the MI whisker region (Brecht et al., 2004). In addition, the PC and CL nuclei project to regions in the dorsolateral neostriatum that receive corticostriatal projections from the MI whisker representation (Berendse and Groenewegen, 1991; Hoffer and Alloway, 2001). Such connections permit the PC and CL nuclei to activate segregated processing streams in the basal-ganglia-thalamocortical circuits (Groenewegen and Berendse, 1994). Although the role of the PC and CL nuclei with respect to whisking behavior is speculative, their connections with cortical regions involved in cognitive awareness, as well as the fact that PC and CL lesions in rats produce deficits in working memory (Burk and Mair, 2001), suggests that these thalamic nuclei rely on recent sensory memories to regulate the moment-to-moment coordination of bilateral whisking behavior.

Contralateral corticothalamic terminals represent modulators

The basis for classifying thalamic afferents as drivers or modulators has been derived from a number of anatomic and physiologic characteristics. Thalamic drivers have large synaptic terminals and do not innervate the reticular nucleus (Sherman and Guillery, 2001), and this is consistent with the morphology and functional role of the ascending afferent projections to sensory-specific thalamic nuclei such as the lateral geniculate body and the ventrobasal complex. By comparison, descending feedback projections from primary sensory cortex to these sensory-specific nuclei have small terminals and collateral branches that innervate the reticular nucleus. These corticothalamic feedback projections are called modulators because they may gate the transmission of sensory information to cortex, but they do not alter the message that is conveyed by the thalamocortical projections (Sherman and Guillery, 2001). Corticothalamic projections from primary sensory cortex to higher-order nuclei such as the POm, however, have large synaptic terminals that resemble drivers (Bourassa et al., 1995). This functional view is further supported by the fact that inactivation of primary somatosensory cortex suppresses stimulus-induced activation of POm neurons (Diamond et al., 1992).

Despite some ambiguity in the available evidence, most of the data suggest that the MI projections to the contralateral thalamus should be classified as modulators. Although MI projections to the ipsilateral VM and VL are considered feedback modulators, the projections to the contralateral VM and VL nuclei do not satisfy this scheme because there are no feedforward projections from VM and VL to the contralateral MI cortex. Likewise, projections from MI to the AM and intralaminar nuclei on the contralateral side do not satisfy a simple feedback scheme. Inspection of the ipsilateral reticular nucleus revealed MI projections to its rostral part, but we never observed any labeled projections to the reticular nucleus on the contralateral side.

Several pieces of data, however, support a modulatory role for the MI projections to the contralateral thalamus. Foremost among these, the MI projections to the AM, VM, and intralaminar nuclei on both sides of the thalamus are characterized by relatively thin axons with small terminal boutons and varicosities. Furthermore, our retrograde labeling experiments confirmed a previous study showing that the rostral part of the reticular nucleus projects to the AM, VM, VL, and intralaminar nuclei on the contralateral side of the thalamus (Raos and Bentivoglio, 1993). Hence, consistent with evidence that ipsilateral feedback projections engage the inhibitory networks of the reticular nucleus, the MI projections to the contralateral thalamus are accompanied by a parallel disynaptic pathway that includes midline-crossing projections from the reticular nucleus to the same targets in the contralateral thalamus. Finally, our retrograde tracing experiments also showed that the MI projections to the contralateral

thalamus originate exclusively from layer VI, a laminar location that is consistent with all other corticothalamic modulator systems that have been described (Sherman and Guillery, 2001). Therefore, we conclude that the MI projections to the contralateral thalamus should be classified as modulators. The precise role of these presumed modulators, however, must await future studies that examine the physiological actions of these connections and their effects on thalamocortical transmission.

Technical considerations

Several findings argue against the possibility that MI projections to the contralateral thalamus represent false positives in which thalamocortical neurons that project to MI cortex also have axonal collaterals that project to the contralateral thalamus. After placing the anterograde tracer BDA into the MI whisker region, the number of retrogradely-labeled neurons in the ipsilateral thalamus was too small to account for the dense terminal labeling observed in the contralateral thalamus. We also found that thalamic injections of a retrograde tracer (ie., FG) failed to reveal any labeled neurons in contralateral thalamic nuclei such as AM, VM, VL, or the intralaminar nuclei. Furthermore, an earlier study used kainic acid to destroy neurons in MI cortex (Molinari et al., 1985), and found that subsequent injections of HRP into the same MI site revealed numerous labeled neurons in the ipsilateral thalamus, but produced no anterograde or retrograde labeling in the contralateral thalamus. Hence, thalamocortical neurons that project to MI do not send axonal collaterals to the contralateral thalamus.

Some of the observed projections to the contralateral thalamus may have been due to tracer diffusion into regions that surround MI cortex. Tracer injected into the MI vibrissal region may have inadvertently diffused more ventrally into the anterior cingulate cortical area, which projects to the MD nucleus in the contralateral thalamus (Negyessy et al., 1998). Although this possibility can not be ruled out, we observed few labeled terminals in the contralateral MD nucleus. By contrast, we observed dense projections to the contralateral AM, VM, and intralaminar nuclei, which are similar to previous findings (Molinari et al., 1985; Rouiller et al., 1991).

In the dual tracing experiments we observed labeled corticothalamic terminals in close proximity to the labeled soma of thalamocortical projection neurons, but this does not prove that the labeled terminals make synaptic contacts with the labeled neurons. Ultrastructural examination with electron microscopy is always necessary to verify synaptic contacts between identified processes. Nonetheless, synaptic contacts can not exist unless they are in close proximity, and our observations with light microscopy demonstrate the feasibility of an interhemispheric cortico-thalamo-cortical route that might interconnect the two MI whisker regions.

Acknowledgements

NIH grants NS37532 and NS052689

Abbreviations in Figures

AD
: anterodorsal nucleus

PC
: paracentral nucleus

AM
: anteromedial nucleus

POm

	posterior nucleus, medial
AV	anteroventral nucleus
PT	paratenial nucleus
CM	centromedial nucleus
PVA	paraventricular nucleus
CL	centrolateral nucleus
Re	reuniens nucleus
CP	caudate-putamen
Ret	Reticular nucleus
f	fornix
Rh	Rhomboid nucleus
G	gelatinosus nucleus
sm	stria medularis
GP	globus pallidus
st	stria terminalis
IAM	interanteromedial nucleus
VL	ventrolateral nucleus
ic	internal capsule
VM	ventromedial nucleus
LD	laterodorsal nucleus

VPM
ventroposteromedial nucleus

MD
mediodorsal nucleus

VPL
ventroposterolateral nucleus

mt
mammillothalamic tract

ZI
zona incerta

LITERATURE CITED

Aggleton JP, Hunt PR, Nagle S, Neave N. The effects of selective lesions within the anterior thalamic nuclei on spatial memory in the rat. Behav Brain Res 1996;81:189–198. [PubMed: 8950016]

Aggleton JP, Brown MW. Episodic memory, amnesia, and the hippocampal-anterior thalamic axis. Behav Brain Sci 1999;22:425–444. [PubMed: 11301518]

Aldes LD. Thalamic connectivity of rat somatic motor cortex. Brain Res Bull 1988;20:333–348. [PubMed: 2452673]

Alloway KD, Hoffer ZS, Hoover JE. Quantitative comparisons of the topographic organization in the ventrobasal complex and posterior nucleus of the rodent thalamus. Brain Res 2003;968:54–68. [PubMed: 12644264]

Alloway KD, Mutic JJ, Hoover JE. Divergent corticostriatal projections from a single cortical column in the somatosensory cortex of rats. Brain Res 1998;785:341–346. [PubMed: 9518681]

Angaut P, Cicirata F, Serapide F. Topographic organization of the cerebellothalamic projections in the rat: An autoradiographic study. Neuroscience 1985;15:389–401. [PubMed: 4022330]

Arbuthnott GW, MacLeod NK, Maxwell DJ, Wright AK. Distribution and synaptic contacts of the cortical terminals arising from neurons in the rat ventromedial thalamic nucleus. Neuroscience 1990;38:47–60. [PubMed: 2175021]

Beckstead RM. An autoradiographic examination of cortico-cortical and subcortical projections of the mediodorsal projection (prefrontal) cortex in the rat. J Comp Neurol 1979;184:43–62. [PubMed: 762282]

Bentivoglio M, Macchi G, Albanese A. The cortical projections of the thalamic intralaminar nuclei, as studied in cat and rat with the multiple fluorescent retrograde tracing technique. Neurosci Lett 1981;26:5–10. [PubMed: 6270605]

Berendse HW, Groenewegen HJ. Restricted cortical termination fields of the midline and intralaminar thalamic nuclei in the rat. Neuroscience 1991;42:73–102. [PubMed: 1713657]

Berman N, Payne BR. Contralateral corticofugal projection from the lateral, suprasylvian and ectosylvian gyri in the cat. Exp Brain Res 1982;47:234–238. [PubMed: 7117448]

Blair HT, Lipscomb BW, Sharp PE. Anticipatory time intervals of head-direction cells in the anterior thalamus of the rat: Implications for path integration in the head direction circuit. J Neurophysiol 1997;78:145–159. [PubMed: 9242269]

Bourassa J, Pinault D, Deschenes M. Corticothalamic projections from the cortical barrel field to the somatosensory thalamus in rats: A single-fibre study using biocytin as an anterograde tracer. Eur J Neurosci 1995;7:19–30. [PubMed: 7711933]

Brecht M, Krauss A, Muhammad S, Sinai-Esfahani L, Bellanca S, Margie TW. Organization of rat vibrissa motor cortex and adjacent areas according to cytoarchitectonics, micro-stimulation, and intracellular stimulation of identified cells. J Comp Neurol 2004;479:360–373. [PubMed: 15514982]

Burk JA, Mair RG. Effects of intralaminar thalamic lesions on sensory attention and motor intentiuon in the rat: a comparison with lesions involving frontal cortex and hippocampus. Beh Brain Res 2001;123:49–63.

Carter DA, Fibiger HC. The projections of the entopeduncular nucleus and globus pallidus in rat as demonstrated by autoradiography and horseradish peroxidase histochemistry. J Comp Neurol 1978;177:113–123. [PubMed: 411809]

Chakrabarti S, Alloway KD. Differential origin of projections from SI barrel cortex to the whisker representation in SII and MI. J Comp Neurol 2006;498:624–636. [PubMed: 16917827]

Deniau JM, Menetrey A, Thierry AM. Indirect nucleus accumbens input to the prefrontal cortex via the substantia nigra pars reticulata: A combined anatomical and electrophysiological study in the rat. Neuroscience 1994;61:533–545. [PubMed: 7526269]

Desbois C, Villanueva L. The organization of lateral ventromedial thalamic connections in the rat: A link for the distribution of nociceptive signals to widespread cortical regions. Neuroscience 2001;102:885–898. [PubMed: 11182250]

De Vito JL. Projections from the cerebral cortex to the intralaminar nuclei in monkey. J Comp Neurol 1969;136:193–202. [PubMed: 4977993]

Diamond ME, Armstrong-James M, Budway MJ, Ebner FF. Somatic sensory responses in the rostral sector of the posterior group (POm) and in the ventral posterior medial nucleus (VPM) of the rat thalamus: dependence on the barrel field cortex. J Comp Neurol 1992;319:66–84. [PubMed: 1592906]

Gao P, Bermejo R, Zeigler HP. Whisker deafferentation and rodent whisking patterns: behavioral evidence for a central pattern generator. J Neurosci 2001;21:5374–5380. [PubMed: 11438614]

Goldman PS. Contralateral projections to the dorsal thalamus from frontal association cortex in the rhesus monkey. Brain Res 1979;166:166–171. [PubMed: 105784]

Groenewegen HJ, Berendse HW. The specificity of the 'nonspecific' midline and intralaminar thalamic nuclei. Trends Neurosci 1994;17:52–57. [PubMed: 7512768]

Groenewegen, HJ.; Witter, MP. Thalamus. In: Paxinos, G., editor. The Rat Nervous System. 3. Elsevier; New York: 2004. p. 407-453.

Guillery RW. Anatomical evidence concerning the role of the thalamus in corticocortical communication: a brief review. J Anat 1995;187:583–592. [PubMed: 8586557]

Guillery RW, Sherman MS. Thalamic relay functions and their role in corticocortical communication: generalizations from the visual system. Neuron 2002;33:1–20. [PubMed: 11779470]

Hall RD, Lindholm EP. Organization of motor and somatosensory neocortex in the albino rat. Brain Res 1974;66:23–38.

Hattox AM, Priest CA, Keller A. Functional circuitry involved in the regulation of whisker movements. J Comp Neurol 2002;442:266–276. [PubMed: 11774341]

Herkenham M. The afferent and efferent connections of the ventromedial thalamic nucleus in the rat. J Comp Neurol 1979;183:487–517. [PubMed: 759445]

Hoffer ZS, Alloway KD. Organization of corticostriatal projections from the vibrissal representations in the primary motor and somatosensory cortical areas of rodents. J Comp Neurol 2001;439:87–103. [PubMed: 11579384]

Hoffer ZS, Arantes H, Roth R, Alloway KD. Functional circuits mediating sensorimotor integration: Quantitative comparisons of projections from rodent barrel cortex to MI cortex, neostriatum, superior colliculus, and pons. J Comp Neurol 2005;488:82–100. [PubMed: 15912501]

Hoogland PV, Wouterlood FG, Welker E, Van der Loos HJ. Ultrastructure of giant and small thalamic terminals of cortical origin: a study of the projections from the barrel cortex in mice using Phaseolus vulgaris leuco-agglutinin (PHA-L). Exp Brain Res 1991;87:159–172. [PubMed: 1721878]

Jones, EG. The Thalamus. Plenum Press; New York: 1985.

Kaitz SS, Robertson RT. Thalamic connections with limbic cortex. II. Cortico-thalamic projections. J Comp Neurol 1981;195:527–545. [PubMed: 7204660]

Kepecs A, Uchida N, Mainen ZF. The sniff as a unit of olfactory processing. Chem Senses 2006;31:167–179. [PubMed: 16339265]

Kincaid AE, Wilson CJ. Corticostriatal innervation of the patch and matrix in the rat neostriatum. J Comp Neurol 1996;374:578–592. [PubMed: 8910736]

Krout KE, Loewry AD, Westby GW, Redgrave P. Superior colliculus projections to midline and intralaminar thalamic nuclei of the rat. J Comp Neurol 2001;431:198–216. [PubMed: 11170000]

Kunzle. Thalamic projections from the precentral motor cortex in Macaca fascicularis. Brain Res 1976;105:253–267. [PubMed: 816421]

Land PW, Simons DJ. Cytochrome oxidase staining in the rat SmI barrel cortex. J Comp Neurol 1985;238:225–235. [PubMed: 2413086]

Leergaard TB, Alloway KD, Pham TA, Bolstad I, Hoffer Z, Pettersen C, Bjaalie JG. Three-dimensional topography of corticopontine projections from rat sensorimotor cortex: Comparisons with corticostriatal projections reveal diverse integrative organization. J Comp Neurol 2004;478:306–322. [PubMed: 15368533]

Leonard CM. The prefrontal cortex of the rat. I. Cortical projection of mediodorsal nucleus. II. Efferent connections. Brain Res 1969;12:321–343. [PubMed: 4184997]

Mitchell BD, Cauller LJ. Corticocortical and thalamocortical projections to layer I of the frontal neocortex in rats. Brain Res 2001;921:68–77. [PubMed: 11720712]

Mitchinson B, Martin CJ, Grant RA, Prescott TJ. Feedback control in active sensing: Rat exploratory whisking is modulated by environmental contact. Proc Roy Soc B 2007;274:1035–1041.

Mizumori SJ, Williams JD. Directionally selective mnemonic properties of neurons in the lateral dorsal nucleus of the thalamus of rats. J Neurosci 1993;13:4015–4028. [PubMed: 8366357]

Molinari M, Minciacchi D, Bentivoglio M, Macchi G. Efferent fibers from the motor cortex terminate bilaterally in the thalamus of rats and cats. Exp Brain Res 1985;57:305–312. [PubMed: 3972032]

Neafsey EJ, Bold EL, Haas G, Hurley-Gius KM, Quirk G, Sievert CF, Terreberry RR. The organization of the rat motor cortex: a microstimulation mapping study. Brain Res 1986;396:77–96. [PubMed: 3708387]

Negyessy L, Hamori J, Bentivoglio M. Contralateral cortical projection to the mediodorsal thalamic nucleus: origin and synaptic organization in the rat. Neuroscience 1998;84:741–753. [PubMed: 9579780]

Ohara PT, Havton LA. Dendritic architecture of rat somatosensory thalamocortical projection neurons. J Comp Neurol 1994;341:159–171. [PubMed: 8163721]

Paxinos, G.; Watson, C. The Rat Brain in Stereotaxic Coordinates. 2. Academic Press; New York: 1986.

Payne BR, Berman N. Contralateral corticofugal projections to cat visual thalamus. Exp Brain Res 1984;53:462–466. [PubMed: 6705875]

Raos V, Bentivoglio M. Crosstalk between the two sides of the thalamus through the reticular nucleus: A retrograde and anterograde tracing study in the rat. J Comp Neurol 1993;332:145–154. [PubMed: 8331209]

Reep RL, Winans SS. Efferent connections of dorsal and ventral agranular insular cortex in the hamster Mesocricetus Auratus. Neuroscience 1982;7:2609–2635. [PubMed: 7155344]

Reichova I, Sherman SM. Somatosensory corticothalamic projections: Distinguishing drivers from modulators. J Neurophysiol 2004;92:2185–2197. [PubMed: 15140908]

Rouiller EM, Liang F, Moret V, Wiesendanger M. Patterns of corticothalamic terminations following injections of *Phaseolus vulgaris* leucoagglutinin (PHA-L) in the sensorimotor cortex of the rat. Neuro Lett 1991;125:93–97.

Sachdev RN, Berg RW, Champney G, Kleinfeld D, Ebner FF. Unilateral vibrissa contact: changes in amplitude but not timing of rhythmic whisking. Somatoses Mot Res 2003;20:163–169.

Sakai ST, Tanaka D. Contralateral corticothalamic projections from area6 in the raccoon. Brain Res 1984;299:371–375. [PubMed: 6733457]

Seki M, Zyo K. Anterior thalamic afferents from the mamillary body and the limbic cortex in the rat. J Comp Neurol 1984;229:242–256. [PubMed: 6438191]

Sellien H, Eshenroder DS, Ebner FF. Comparison of bilateral whisker movement in freely exploring and head-fixed adult rats. Somatosens Mot Res 2005;22:97–114. [PubMed: 16338819]

Sherman SM, Guillery RW. On the action that one nerve cell and have on another: Distinguishing “drivers” from “modulators”. Proc Natl Acad Sci USA 1998;95:7121–7126. [PubMed: 9618549]

Sherman, SM.; Guillery, RW. Exploring the Thalamus. San Diego, CA: Academic Press; 2001.

Shibata H. Topographic organization of subcortical projections to the anterior thalamic nuclei in the rat. J Comp Neurol 1992;323:117–127. [PubMed: 1385491]

Shibata H. Efferent projections from the anterior thalamic nuclei to the cingulated cortex in the rat. J Comp Neurol 1993;330:533–542. [PubMed: 8320343]

Shibata H, Naito J. Organization of anterior cingulate and frontal cortical projections to the anterior and laterodorsal thalamic nuclei in the rat. Brain Res 2005;1059:93–103. [PubMed: 16157311]

Sotnichencko TS. Convergence of descending pathways of motor, visual and limbic cortex in the cat di- and mesencephalon. Brain Res 1976;116:401–415. [PubMed: 974784]

Swanson LW, Cowan WM. An autoradiographic study of the organization of the efferent connections of the hippocampal formation in the rat. J Comp Neurol 1977;172:49–84. [PubMed: 65364]

Towal RB, Hartmann MJ. Right-left asymmetries in the whisking behavior of rats anticipate head movements. J Neurosci 2006;26:8838–8846. [PubMed: 16928873]

Van der Werf YD, Witter MP, Groenewegen HJ. The intralaminar and midline nuclei of the thalamus. Anatomical and functional evidence for participation in processes of arousal and awareness. Brain Res Brain Res Rev 2002;39:107–140. [PubMed: 12423763]

Van Groen T, Kadish I, Wyss JM. Efferent connections of the anteromedial nucleus of the thalamus of the rat. Brain Res Brain Res Rev 1999;30:1–26. [PubMed: 10407123]

Villanueva L, Desbois C, Le Bars D, Bernard JF. Organization of diencephalic projections from the medullary subnucleus reticularis dorsalis and the adjacent cuneate nucleus: A retrograde and anterograde tracer study in the rat. J Comp Neurol 1998;390:133–160. [PubMed: 9456181]

Vogt, BA.; Vogt, L.; Farber, NB. Cingulate cortex and disease models. In: Paxinos, G., editor. The Rat Nervous System. 3. Elsevier; New York: 2004. p. 705-727.

Welker WI. Analysis of sniffing in the albino rat. Behaviour 1964;12:223–244.

Witter MP, Ostendorf RH, Groenewegen HJ. Heterogeneity in the dorsal subiculum of the rat: Distinct neuronal zones project to different cortical and subcortical targets. Eur J Neurosci 1990;2:718–725. [PubMed: 12106290]

Wong-Riley M. Changes in the visual system of monocularly sutured or enucleated cats demonstrable with cytochrome oxidase histochemistry. Brain Res 1979;171:11–28. [PubMed: 223730]

Yamamoto T, Noda T, Samejima A, Oka H. A morphological investigation of thalamic neurons by intracellular HRP staining in cats. J Comp Neurol 1985;236:331–347. [PubMed: 2414336]

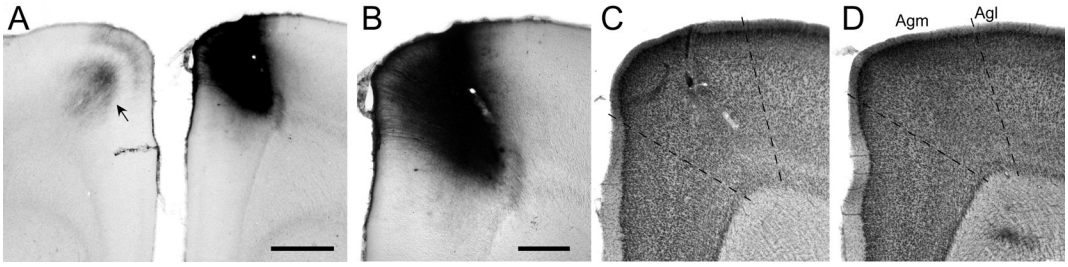

Fig 1.

Location of a BDA deposit in the MI whisker region of rat BN27. **A:** Dense deposit of BDA at a site in the right hemisphere that evoked discrete twitches of whiskers D1, D2, and E2. Callosal projections from the BDA injection site terminated in the corresponding part of the left hemisphere (arrow). Scale, 1 mm. **B:** Magnified view of the BDA injection site. Scale, 500 μm. **C:** An adjacent thionin-stained section reveals slight damage produced by the tracer injection. **D:** Another thionin-stained section, located 160 μm caudal to the section in panel C, reveals the cytoarchitectonic distinctions between medial (Agm) and lateral (Agl) agranular cortex. Panels C and D shown at the same magnification as panel B.

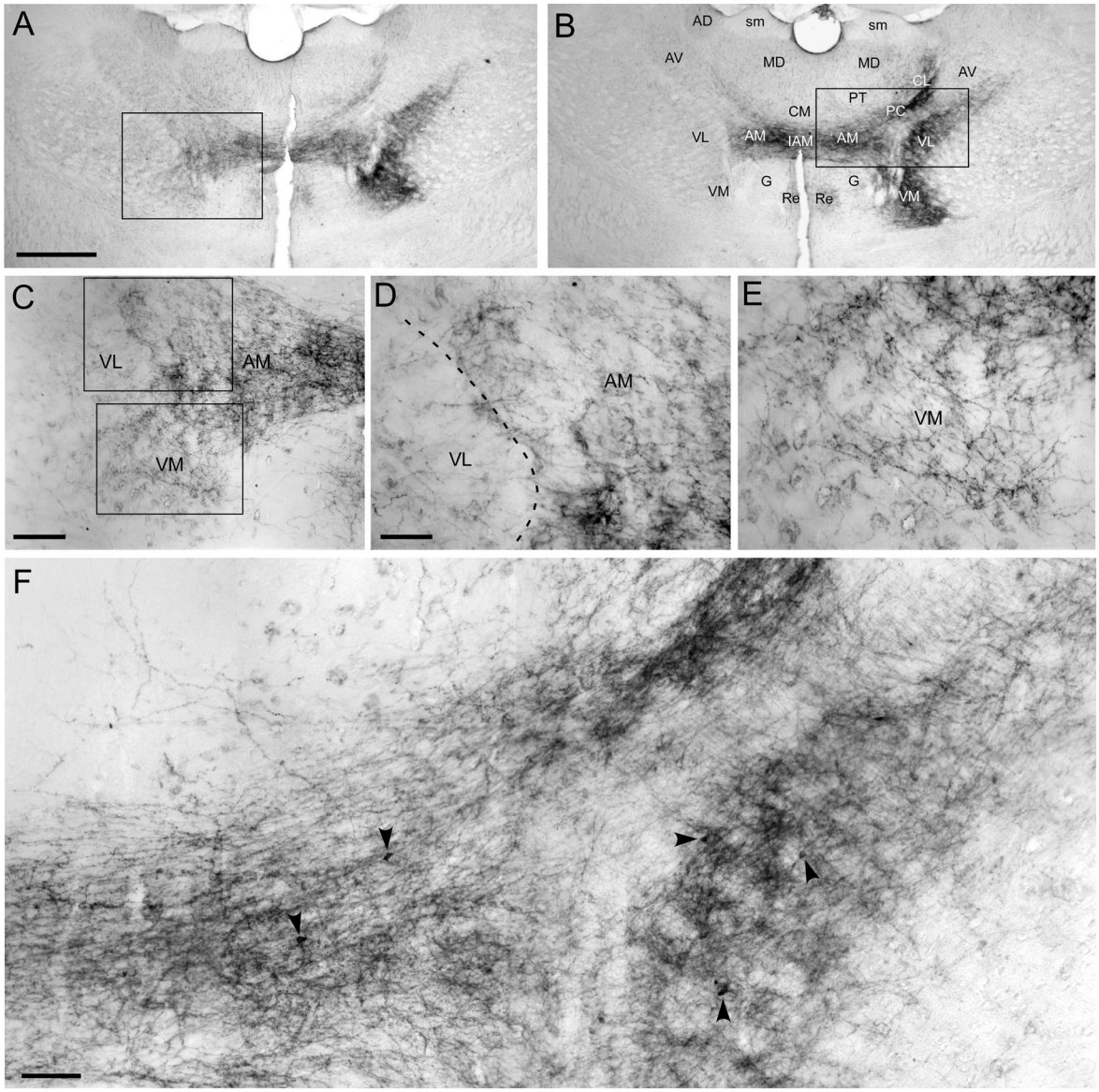

Fig. 2.

Bilateral corticothalamic projections from the MI whisker region in rat BN27. **A, B:** Low power views of BDA-labeled terminals in the thalamus; panel B is 160 μm caudal to panel A. Rectangles in panels A and B indicate the regions in panels C and F, respectively. Scale, 1.0 mm; panels A and B at same magnification. **C:** Labeled terminals in AM, VL, and VM. Rectangles indicate photomicrographs appearing in panels D and E. Scale, 250 μm. **D:** Detailed view of labeled terminals in AM and the medial part of VL. Scale, 100 μm. **E:** Detailed view of labeled terminals in nucleus VM. Same magnification as panel D. **F.** Collage showing detailed view of BDA labeling in the ipsilateral thalamus. Arrows indicate retrogradely-labeled cells, all other regions of dense BDA labeling represent anterogradely-labeled terminals. Scale, 100 μm.

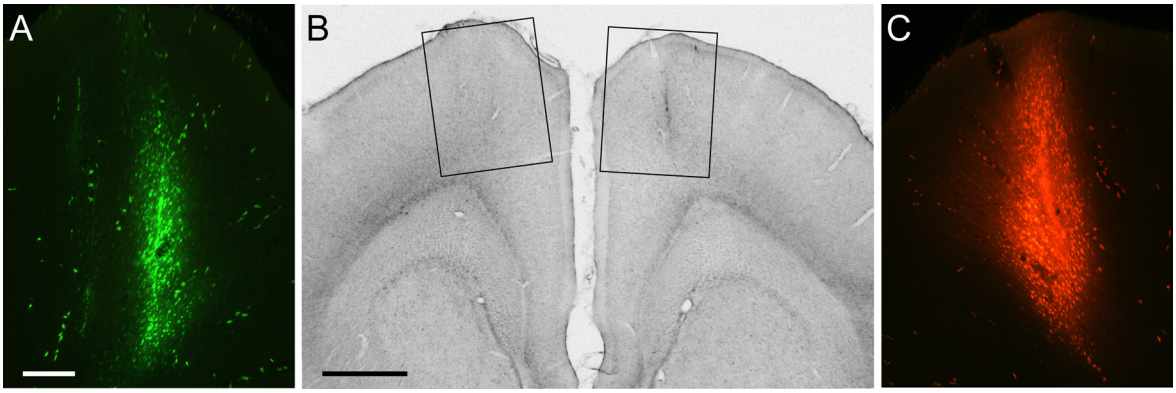

Fig. 3.

Bilateral injections of Alexa-Fluoro (AF) and Fluoro-Ruby (FR) into the MI whisker regions of rat BN11. **A:** View of the AF injection site in which ICMS evoked twitches of whisker B2. Scale, 250 μm. **B:** Location of the AF and FR tracer injection sites in the left and right hemispheres, respectively, as seen during light microscopy. Rectangles indicate the regions appearing in panels A and C during fluorescent microscopy. Scale, 1.0 mm. **C:** View of the FR injection site in which ICMS evoked twitches of whisker B1. Magnification same as panel A. A copy of the figure using magenta-green coloring is available as a supplementary figure.

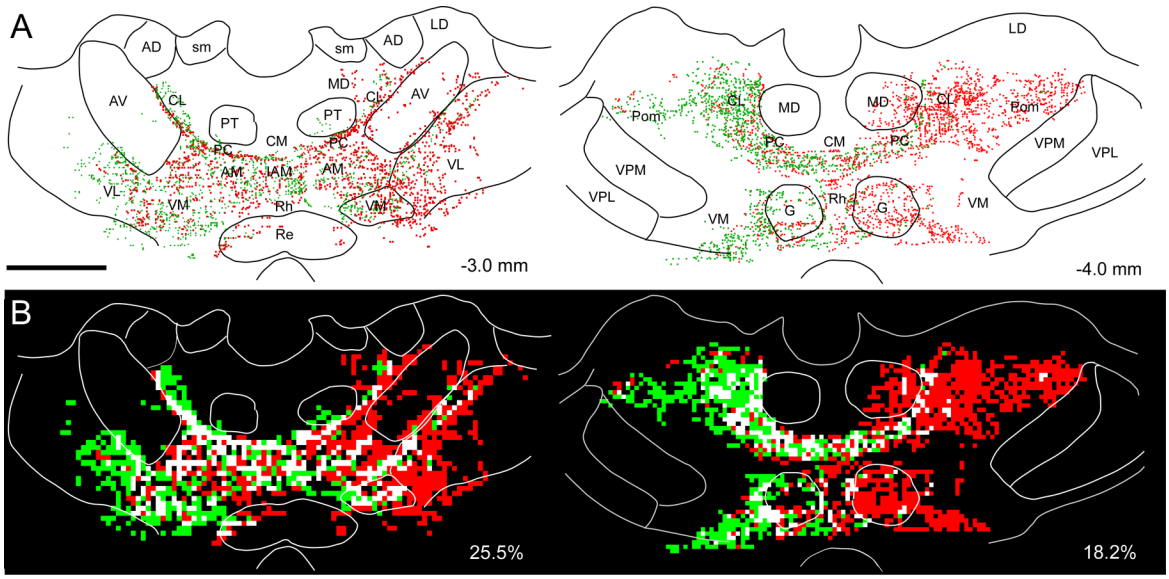

Fig. 4.

Bilateral distribution of AF- and FR-labeled corticothalamic terminal projections from the MI whisker regions in rat BN11. **A:** Reconstructed coronal sections depict the boundaries of several thalamic nuclei with respect to terminal varicosities labeled by AF (green dots) or FR (red dots). The distance from bregma is shown at lower right for each section. **B:** Overlap analysis of the reconstructions shown in panel A. After subdividing the reconstructions into a grid of 50 μm^2 bins, the bins are colored green and red according to the presence of AF- and FR-labeled varicosities. White bins indicate regions occupied by terminal projections from both MI tracer injections. Scale bar = 1 mm for both panels. A copy of the figure using magenta-green coloring is available as a supplementary figure.

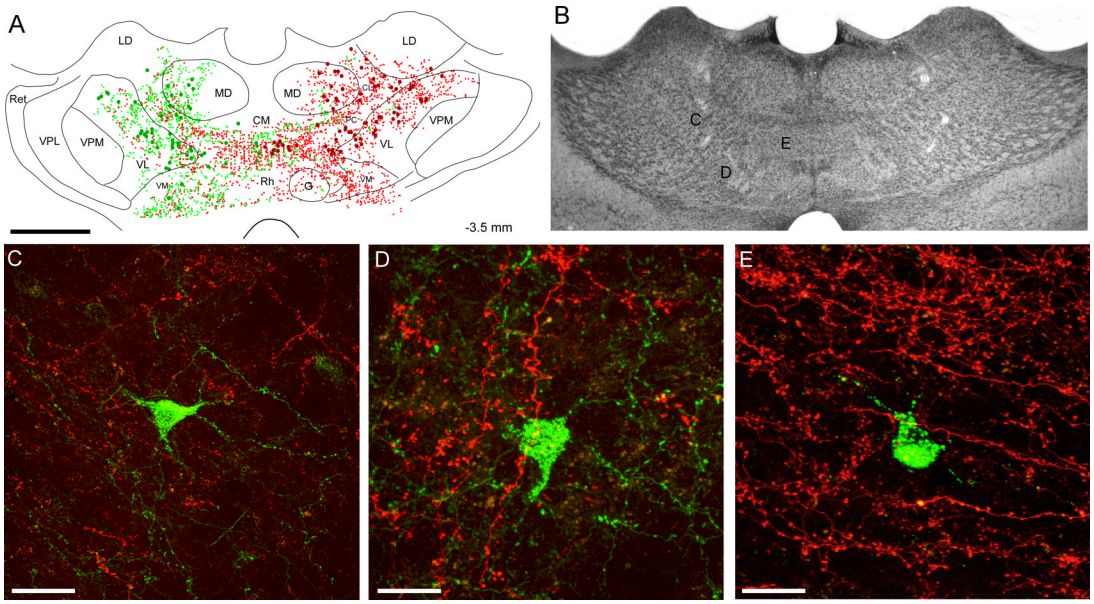

Fig. 5.

Bilateral distribution of AF- and FR- labeled terminals and soma in rat BN11. **A:** Reconstruction of labeled terminals (small dots) and cell bodies (large filled circles) in a coronal section located halfway between the coronal sections appearing in Fig. 4. Scale, 1 mm. **B:** Thionin-stained section located adjacent to the section reconstructed in panel A. Letters indicate the approximate location of the regions shown in panels C, D, and E. Same scale as in panel A. **C, D, E:** FR-labeled corticothalamic projections from the right MI whisker region are intermingled with AF-labeled thalamocortical neurons that project to the left MI whisker region. Scale bars, 40 μm in panel C, 20 μm in panels D and E. A copy of the figure using magenta-green coloring is available as a supplementary figure.

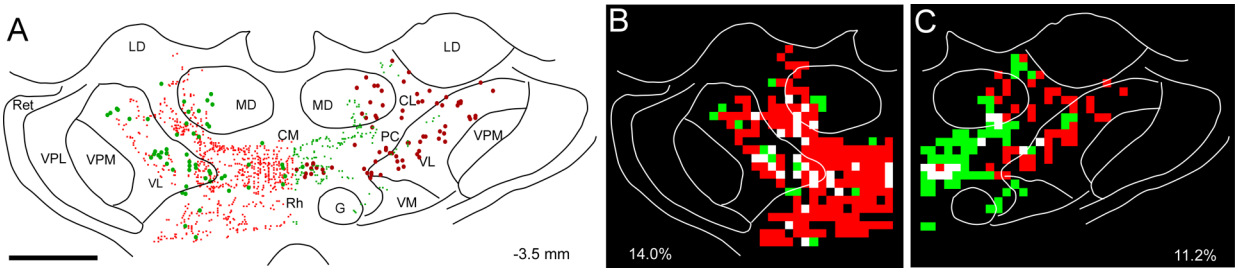

Fig. 6.

Proximity of labeled corticothalamic projections with respect to thalamocortical neurons labeled by the other tracer. **A.** Reconstruction of labeled corticothalamic terminals in the contralateral thalamus shown with respect to retrogradely-labeled soma in case BN11. Only contralaterally-labeled corticothalamic projections are shown, the locations of the ipsilaterally-labeled corticothalamic projections have been removed. Scale, 1 mm. **B.** Overlap analysis of FR-labeled terminals and AF-labeled neurons after subdividing the left half of the thalamic reconstruction into an array of 100 μm^2 bins. Green bins contain AF-labeled neurons, red bins contain AF-labeled terminals, white bins contain both neurons and terminals. Percentage indicates the proportion of labeled bins that are white. C. Overlap analysis of AF-labeled terminals and FR-labeled neurons in the right half of the same thalamic section shown in panel A. A copy of the figure using magenta-green coloring is available as a supplementary figure.

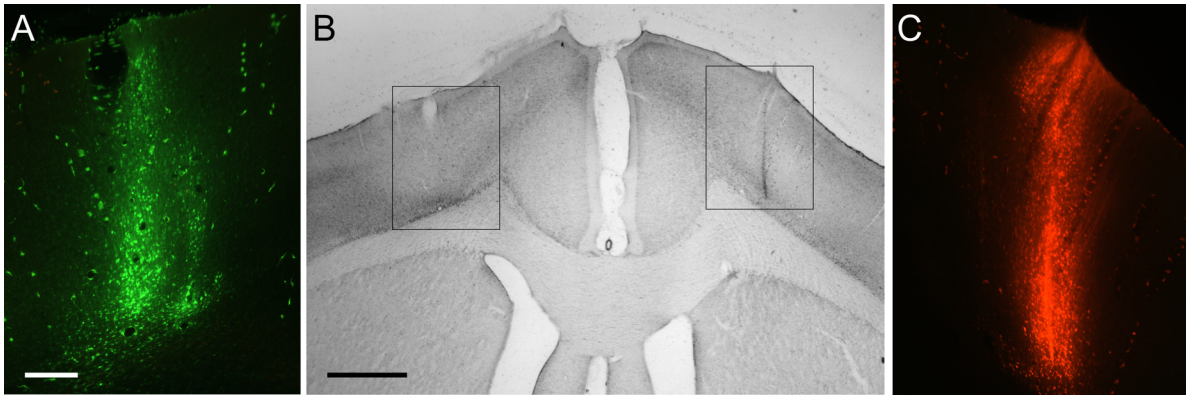

Fig. 7.

Bilateral injections of Alexa-Fluoro (AF) and Fluoro-Ruby (FR) into the MI forepaw regions of rat BN16. **A:** View of the AF injection site in which ICMS evoked twitches of the right forepaw. Scale, 250 μm. **B:** Location of the AF and FR tracer injection sites in the left and right hemispheres, respectively, as seen during light microscopy. Rectangles indicate the regions appearing in panels A and C during fluorescent microscopy. Scale, 1.0 mm. **C:** View of the FR injection site in which ICMS evoked twitches of the left forepaw. Magnification same as panel A. A copy of the figure using magenta-green coloring is available as a supplementary figure.

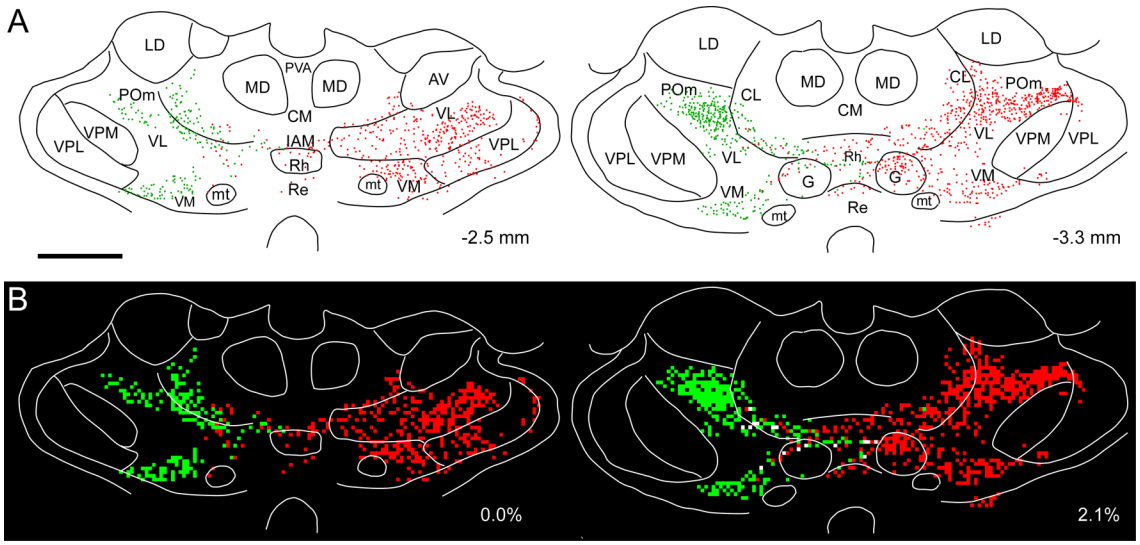

Fig. 8.

Bilateral distribution of AF- and FR-labeled corticothalamic terminal projections from the MI forepaw regions in rat BN16. Reconstructions of the labeling patterns (**A**) and the corresponding overlap analysis (**B**) are presented as in Figure 4. Scale bar = 1 mm for both panels. A copy of the figure using magenta-green coloring is available as a supplementary figure.

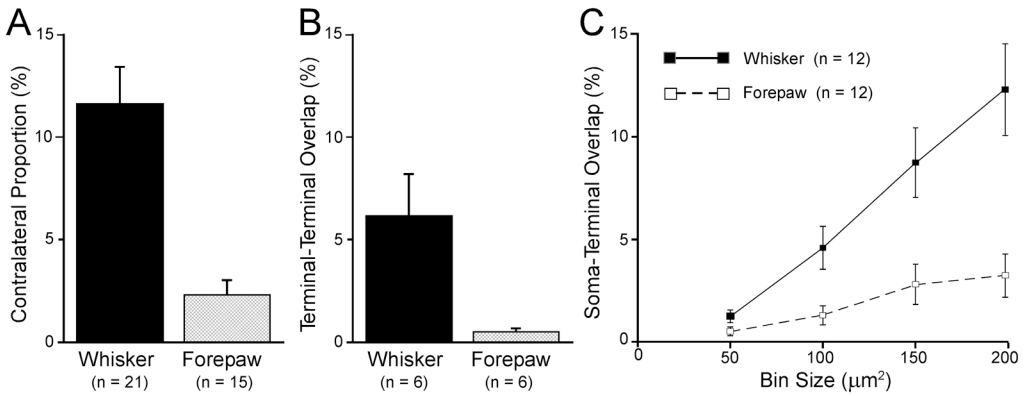

Fig. 9.

Quantitative analysis of corticothalamic projections from the whisker and forepaw regions in MI. **A:** Proportion of corticothalamic labeling that occupied the side of the thalamus located contralateral to the tracer injection in MI. Data based on the number of 50 μm^2 bins that contained labeled varicosities (see Methods). **B:** Amount of tracer overlap in thalamus following bilateral injections of different tracers into MI of each hemisphere. Data based on the number of 50 μm^2 bins that contained both AF- and FR-labeled terminals. **C:** Amount of tracer overlap on each side of the thalamus in which a labeled terminal occupied the same bin that contained a soma labeled by the other tracer.

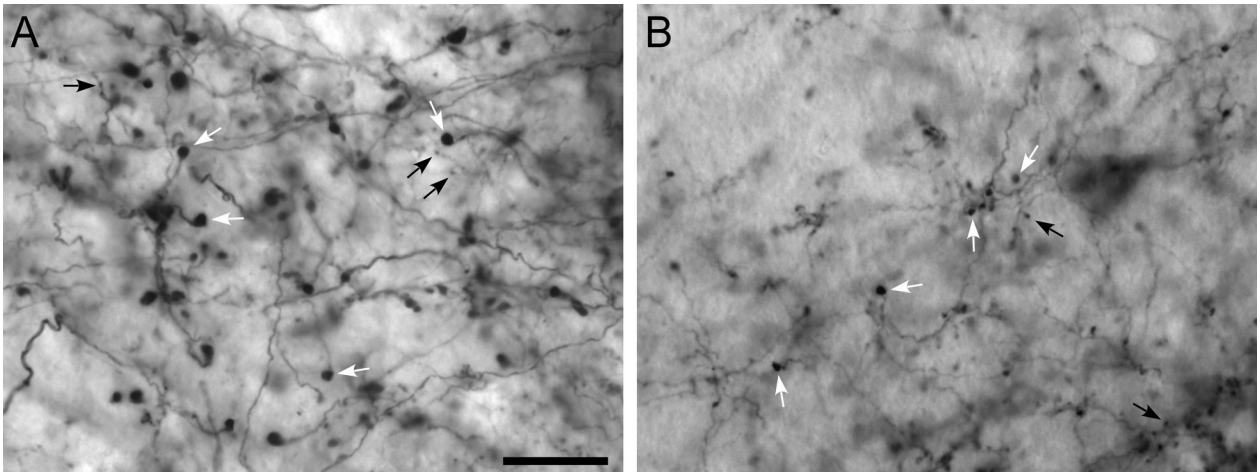

Fig. 10.

Comparison of BDA-labeled corticothalamic projections from SI and MI to the ipsilateral nucleus POm. **A:** Labeled terminals in the ipsilateral Pom after injecting BDA into SI barrel cortex. Black arrows indicate small, modulator terminals; white arrows indicate large, driver terminals. Scale, 25 μm. **B:** Labeled terminals in the ipsilateral POm after injecting BDA into the MI whisker region. Arrows and scale are presented as in panel A.

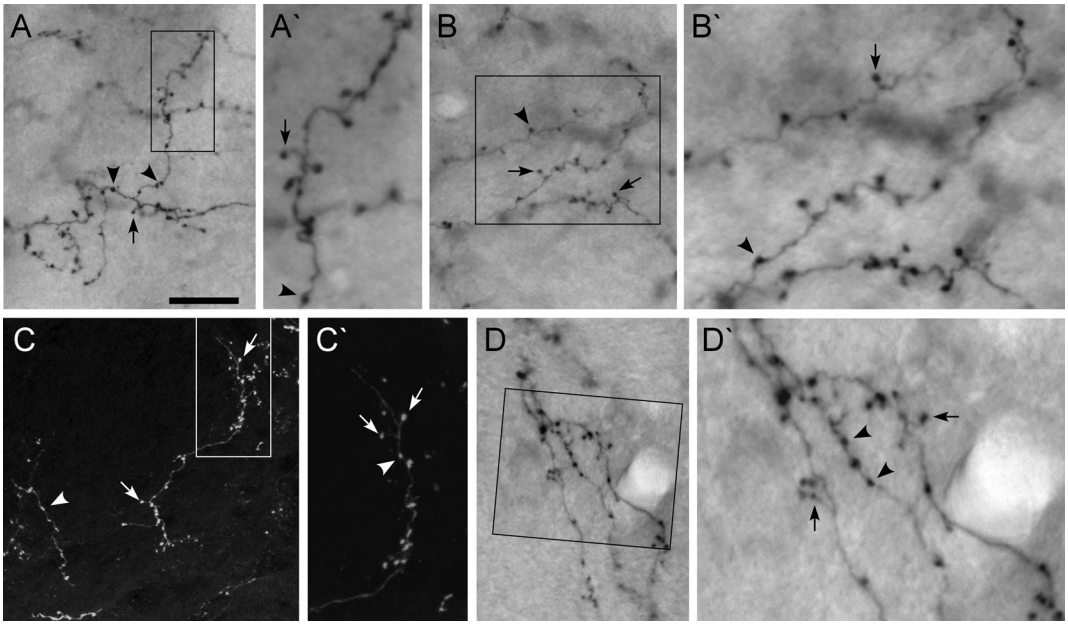

Fig. 11.

Comparison of labeled terminal projections from MI to the contralateral thalamus. **A, A′**: BDA-labeled terminals in the contralateral nucleus AM. **B, B′**: BDA-labeled terminals in the contralateral nucleus VL. **C, C′**: FR-labeled terminals in the contralateral nucleus VM. **D, D′**: BDA-labeled terminals in the contralateral nucleus VM. Arrows indicate “drumstick-shaped” varicosites and arrowheads indicate “beaded enlargements.” Rectangles in panels A, B, C and D, indicate regions depicted at higher magnification in panels A′, B′, C′, and D′. Scale bar represents 25 μm for panels A, B, C, and D, but represents 10 μm for panels A′, B′, C′, and D′.

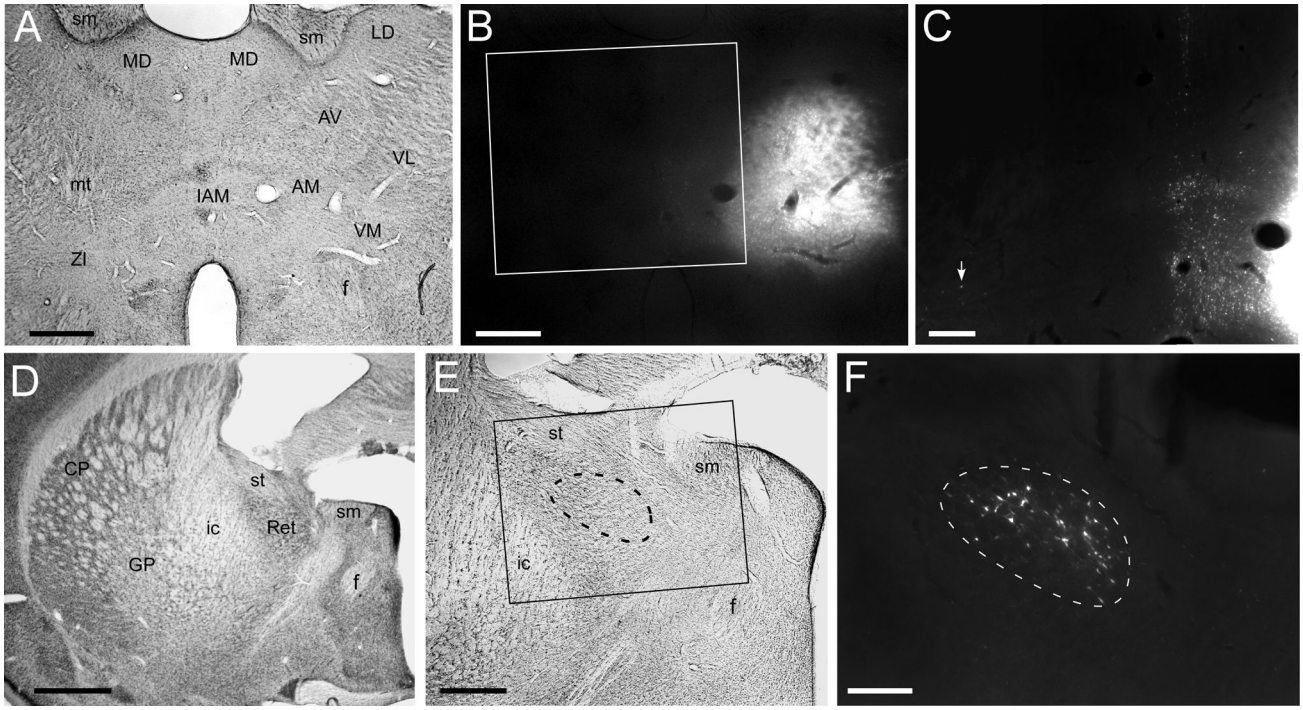

Fig. 12.

Thalamic labeling produced by depositing fluoro-gold (FG) into nuclei AV, AM, VM, and VL. **A:** Location of FG injection site 2 mm posterior to bregma. Scale, 500 μm; panels A and B at same magnification. **B:** Section in panel A viewed during fluorescent microscopy, rectangle indicates region in panel C. **C:** Neurons retrogradely labeled by FG appear along midline ipsilateral to the FG injection site but were not apparent in the contralateral thalamus except for a small number in the zona incerta (arrow). Scale, 250 μm. **D:** Thionin stained section through rostral part of the reticular nucleus. Scale, 1 mm. **E:** Adjacent unstained section shows magnified view of rostral reticular nucleus. Rectangle and dashed contour indicate regions appearing in panel F. Scale, 500 μm. **F:** Section in panel E viewed during fluorescent microscopy shows cluster of FG-labeled neurons in the reticular nucleus. Scale, 250 μm.

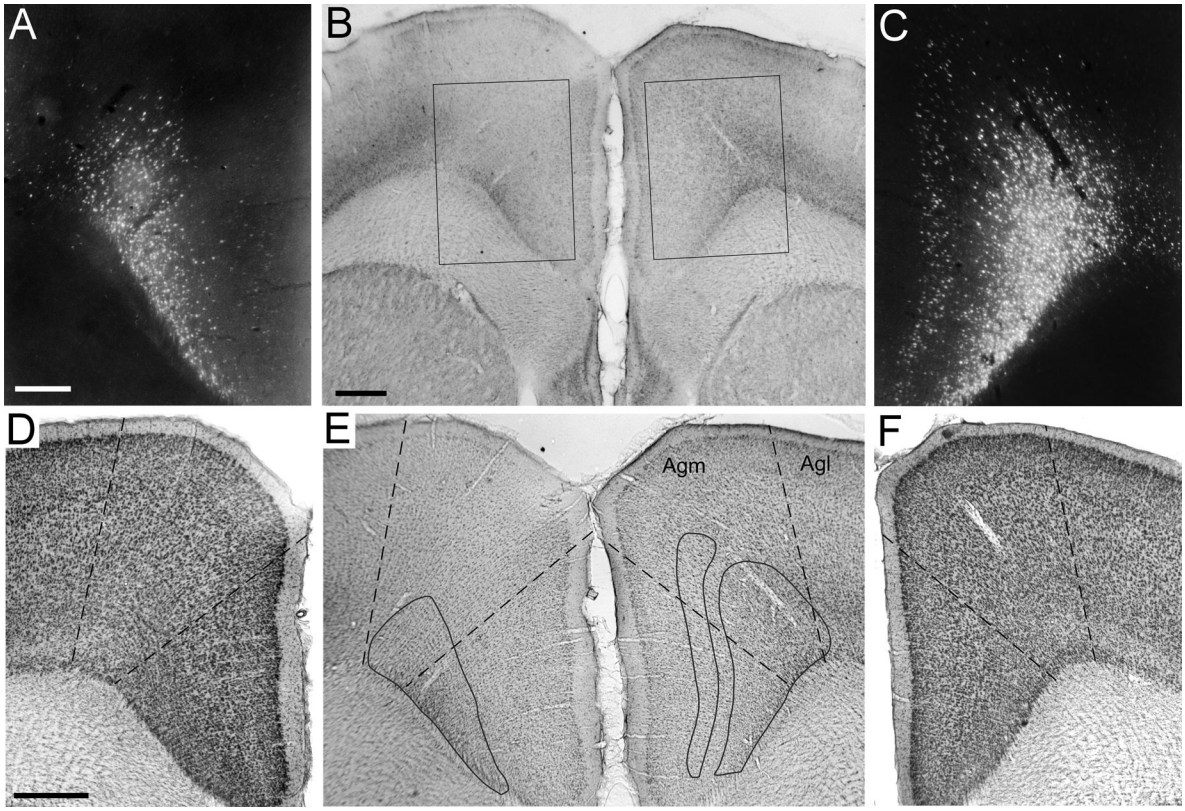

Fig. 13.

Labeled neurons in MI cortex produced by a deposit of FG in the right thalamus. **A:** Retrogradely-labeled neurons in deep layer VI of the contralateral MI cortex. Scale, 250 μm. **B:** Unstained section through the left and right MI cortices; rectangles indicate the regions shown in panels A and C. Scale, 500 μm. **C:** Retrogradely labeled neurons in layers Vb and VI of the ipsilateral MI cortex. Same magnification as panel A. **D:** Thionin-stained section through left MI cortex located adjacent to the section in panel A. Dashed lines indicate the borders of the medial agranular (Agm) cortex. Scale, 500 μm. **E:** Same section as in panel B but shown at magnification used for panels D and F. Solid contours show locations of retrogradely-labeled neurons after superimposing the fluorescent photomicrographs in A and C onto the section. Dashed lines show approximate Agm borders after superimposing the thionin-stained sections in panels D and F onto the section. **F:** Thionin-stained section through right MI cortex located adjacent to the section in panel C. Dashed lines and magnification are shown as in panel D.

Table 1

Summary of Tracer Injections in MI Cortex

Case #	Left Hemisphere		Right Hemisphere	
	Tracer[a]	Region[b]	Tracer[a]	Region[b]
BN2			BDA (3)	Wh-C2
BN3			BDA (3)	Wh-B2 C2
BN7			BDA (2)	Wh-C3 D2,3
BN9	AF (1)	Wh-B1,2	FR (1)	Wh-C2
BN11	AF (1)	Wh-B2	FR (1)	Wh-B1
BN12	AF (1)	Wh-C2,3	FR (1)	Wh-C2
BN13	FR (1)	Wh-D2	AF (1)	Wh-D2 E2
BN15	AF (1)	Fp	FR (1)	Fp
BN16	AF (1)	Fp	FR (1)	Fp
BN19			BDA (2)	Wh-A1
BN20			BDA (2)	Wh-B2
BN21			BDA (2)	Fp
BN22			FR (1)	Fp
BN23			FR (1)	Fp
BN24			BDA (2)	Wh-B1
BN25			FR (1)	Wh-C1
BN26	AF (1)	Fp	FR (1)	Fp
BN27			BDA (3)	Wh-D1,2 E2
BN28	AF (1)	Fp	FR (1)	Fp
BN29	AF (1)	Fp	FR (1)	Fp
BN30	AF (1)	Wh-D1,2	FR (1)	Wh-C1 D1
BN31	AF (1)	Wh-D1	FR (1)	Wh-D1,2
BN33	AF (1)	Fp	FR (1)	Fp
BN35			BDA (1)	Wh-C1,2

[a] Values in parentheses represent number of injection penetrations

[b] Wh indicates whiskers, Fp indicates forepaw